

Eddies around Madagascar — the retroflexion re-considered

Quartly, G.D., J.J.H. Buck[†], M.A. Srokosz and A.C. Coward

*National Oceanography Centre, Southampton
Southampton, Hants, SO14 3ZH, UK*

(accepted by *Journal of Marine Systems* 16th June 2006)

Abstract

The Agulhas Current with its retroflexion and attendant eddy-shedding is the cause of some of the greatest mesoscale variability in the ocean. This paper considers the area to the south and east of Madagascar, which provides some of the source waters of the Agulhas Current, and examines the propagating sea surface height signals in altimetry and output from a numerical model, OCCAM. Both show bands of variability along the axis of the East Madagascar Current (EMC) and along a zonal band near 25°S. Sequences of images plus associated temperature data suggest that a number of westward-propagating eddies are present in this zonal band. The paper then focuses on the region to the south of the island, where ocean colour and infra-red imagery are evocative of an East Madagascar Retroflexion. The synthesis of data analysed in this paper, however, show that remotely observed features in this area can be explained by anticyclonic eddies moving westward through the region, and this explanation is consistent with numerical model output and the trajectories of drifting buoys.

Keywords: Retroflexion, eddies, biophysical interactions, upwelling, current variability

Regional index terms: Western Indian Ocean, Agulhas Current system, East Madagascar Current

1. Introduction

The flow regime to the south of Madagascar has been likened to that south of South Africa. The Agulhas Current flows poleward along the east coast of South Africa as one of the strongest western boundary currents in the world (Stramma and Lutjeharms, 1997; de Ruijter et al., 1999). The current lies close to the coast until Port Alfred (27°E, 34°S), after this the shelf edge broadens forcing the deep current further offshore. However, the Agulhas Current does not continue around the southern point following some deep isobath; rather, it is carried southward by inertia, and then retroflects (turns back on itself) to flow eastward in response to the change in potential vorticity (de Ruijter and Boudra, 1985). This Agulhas Retroflexion is not stable, but from time to time moves westwards, until instabilities in the flow lead to the pinching off of an Agulhas ring and the reformation of the retroflexion further east (Lutjeharms and van Ballegooyen, 1988).

The East Madagascar Current (EMC) flowing poleward along the eastern edge of Madagascar may be considered a mini western boundary current (Fig. 1a). A number of papers have alluded to similarities to the Agulhas. Hydrographic measurements are scarce, but transects across the EMC have shown it to be deep, with temperature, velocity and dissolved oxygen showing signals down to 2000m (Swallow et al., 1988; Donohue and Toole, 2003). Schott et al. (1988) deployed moorings across the EMC at 23°S during the period October 1984 to September 1985, and showed that the flow during that time was nearly always southward, apart from for a 3-week period near the beginning of July 1985.

The flow to the south of Madagascar is not clear. Some authors (Gründlingh, 1993; Tomczak and Godfrey, 1994) suggest that the EMC flows due west upon reaching the southern tip of Madagascar. Lutjeharms (1976) found intermediate waters of central Indian Ocean origin on the eastern side of the Mozambique Channel, and concluded that the EMC must, at least partially, hug the Madagascar coastline and head northwards up the west coast of Madagascar for a few hundred kilometres before turning anticlockwise to join the southward flow along the western edge of the Mozambique Channel. This view is certainly complicated by the recent realisation that there is no

permanent southbound Mozambique Current, but rather a series of anticyclonic eddies (Ridderinkhof and de Ruijter, 2003; Schouten et al., 2003).

A third conjecture is that the EMC retroflects to the south of Madagascar i.e. that the majority of the current turns anticyclonically upon itself to head eastward, with the possibility of eddy-shedding from this loop. This was first proposed by Lutjeharms et al. (1981) on the evidence of buoy trajectories, and has been supported by a number of remote-sensing observations (Lutjeharms, 1988; Lutjeharms and Machu, 2000; di Marco et al., 2000; Quartly and Srokosz, 2003a). These have used thermal infra-red and ocean colour imagery, usually single images rather than sequences, to draw parallels with the retroflexion of the Agulhas Current.

The aim of this paper is to understand the eventual destination of the waters of the EMC, using sequences of images to overcome the ambiguity of single images, incorporating information on current anomalies from altimetry, and including insight gained from analysis of numerical model output. Section 2 introduces the various datasets used, with section 3 examining the movement of features to the east of Madagascar in both the altimetry data and model output. In particular we show that the observations along 25°S are strongly indicative of a train of westward-propagating eddies. Section 4 looks at the interaction of these eddies to the south of Madagascar, including the generation of retroflexion-like patterns within temperature and ocean colour imagery. Section 5 brings these findings together into a summary.

2. Data used and pre-processing applied

We have used satellite data from three different sources, plus output from a 0.25° x 0.25° (eddy-permitting) numerical model. These various sources are described briefly below along with any simple pre-processing used for compositing and for removing long-period large-scale variations.

2.1 Altimetric records of Sea Surface Height

Records of sea surface height (SSH) from altimetry can be used to identify highs (anticyclones) and lows (cyclones) and their associated geostrophic currents. We used the MSLA product available from CLS, which was provided at intervals of 10 days on a global 0.25° x 0.25° grid. We analysed data for the period April 1995 to August 2001, constructed from TOPEX/Poseidon and ERS-2 data, which enables a better representation of features than would be obtained from one altimeter alone. Details of CLS's processing, combining and interpolation of the altimeter data are given in Le Traon and Ogor (1998) and Le Traon et al. (1998).

The SSH fields are given relative to a reference mean of 1993-1995, so all features are anomalies relative to an unknown mean circulation. This means that there will be no signal associated with the mean flow of the EMC, but that short-term variations in it (e.g. eddies or meanders) will be apparent.

For a large part of the region of interest the variation in SSH (Fig. 1b) is dominated by the annual steric signal and other large-scale phenomena, which are not of interest in this study. These modes of variability are removed by applying an EOF analysis and subtracting the first 4 modes from the individual composites. This is the technique used by Quartly and Srokosz (2002) on sea surface temperature data and is based on the assumption that large-scale modes common to the whole region will explain more of the variability than the eddy patterns we wish to retain. The analysis is not strongly sensitive to whether 3, 4 or 5 modes are removed. Typically the first three modes represent any residual mean (in this case because the SSH data are referred to the mean of an earlier period) and predominantly seasonal or interannual variations. Fig. 1c shows the r.m.s. variability of the resulting dataset. The principal effect of the filtering is to reduce the variability north of 18°S, which is dominated by long period (seasonal and interannual) variations.

2.2 Chlorophyll concentration from ocean colour

The ocean colour sensor, SeaWiFS, has been operating since Sept. 1997. We obtained the version4 chlorophyll concentrations provided by NASA/GSFC (<http://daac.gsfc.nasa.gov/data/dataset/SEAWIFS>). These are provided daily on a global $0.09^\circ \times 0.09^\circ$ grid. As chlorophyll concentration (CC) follows an approximately log-normal distribution (Campbell, 1995), it is useful to perform analysis in terms of logarithms. We constructed 10-day composites by taking the mean of $\log_{10}(\text{CC})$. There is a seasonal cycle to the chlorophyll values, but the spatial variations associated with coastal upwelling south of Madagascar are always pronounced (see Quartly and Srokosz, 2004), so no further filtering is needed for the analysis shown here.

2.3 Satellite records of sea surface temperature

Our source of sea surface temperature (SST) data is the TRMM Microwave Imager (TMI), a passive microwave sensor able to measure SST through clouds. The data are provided as daily files on a 0.25° grid by Remote Sensing Systems (<http://www.remss.com>), and we have made 10-day composites, coincident with the altimetry and ocean colour composites.

2.4 Numerical output from OCCAM

OCCAM is an eddy-permitting global model run at the National Oceanography Centre, Southampton. General details can be found in Webb et al. (1998) and de Cuevas et al. (1999). It is a z-level model run on a B-grid (velocity vectors calculated at intermediate points to temperature and salinity), and incorporates partially-filled bottom cells to improve the modelling of flow across topography. There are a number of different runs of the model, with different resolutions, numbers of layers and forcing. The data used here are from a version with 0.25° horizontal resolution, 66 depth layers (with finer spacing nearer the surface than at depth), and with momentum, heat and freshwater forcing calculated from NCEP 6-hourly fields and the model's SST, via bulk layer formulations (Coward and de Cuevas, 2005). Evaporation is derived directly from the six-hourly latent heat field, whilst precipitation values are linearly interpolated in time from monthly NCEP fields. There is an additional relaxation of surface salinity values towards the Levitus climatology with a timescale of 30 days. This use of high-frequency realistic data for forcing is important, because it helps guarantee more interannual variability than was noted for its predecessor the Fine Resolution Antarctic Model (FRAM, see Quartly and Srokosz (1993) for an example of the regularity of its eddies, locked to the seasonal cycle of forcing).

The OCCAM data are available as 5-day averages every 5 days for a period of 18 years (corresponding to the forcing fields of 1985 to 2002 inclusive). Prior to the start of this period, the model was spun-up for 4 model years starting from a climatological state. By the end of this initial period, the major circulation features were well established and the small subsequent drift in global mean kinetic energy was less than the seasonal and interannual range of variability. The annual mean transport through Drake Passage was 170 Sv and the model developed a poleward Agulhas Current, with a full-depth annual mean transport of 48 Sv at 30°S (off Durban). This is a little lower than the 70 Sv found by Beal & Bryden (1999) in a one-off transect of this section, but their figure does not include the effect of the deeper counter-current. The sea surface height, a prognostic variable calculated using an explicit non-linear formulation, is the parameter of chief interest here, as that mirrors the altimeter measurements of SSH; however, temperature, salinity and velocity vectors from all layers of the model can be used in the interpretation of the surface data. The OCCAM SSH data are treated similarly to the altimeter data, with data for 1994 to 2001 being selected, and anomalies being determined relative to the 8-year mean, and the first 4 EOF modes then subtracted. This removes some bias variations of up to 5 cm between successive 5-day means, which appear to be caused by large-scale atmospheric pressure systems moving rapidly through the region of interest.

3. Variability in sea surface height

In this section we contrast the SSH signals in the altimeter and model datasets, first starting with the overall pattern of variability in this whole section of the Indian Ocean, and then focussing in on the features approaching the southern end of Madagascar and their interaction with one another.

3.1 Variability in sea surface height

Figures 1c,d show the variability in SSH as recorded separately by altimeter and model output. The patterns are broadly similar, although the amplitude of the variability is less in the model than in the altimetry. One cause of this difference is the measurement and correction errors in the altimetry, which particularly affect variability estimates in quiet regions. Secondly, OCCAM and most other models underestimate the variability in active regions, because they have insufficient variability in the forcing or inadequate resolution to develop the instabilities. It should be noted that the version of OCCAM used here, with both wind-forcing and latent heat fluxes derived from 6-hourly NCEP reanalysis data, exhibits greater variability than previous versions of the model, although the zonal band of variability along 28°S in Fig. 1d is further south than in earlier runs or in the altimetry data. The altimetry (Fig. 1c) shows significant variability on the western side of the Mozambique Channel, especially around 18°-20°S. A similar band of variability is found in OCCAM output (Fig. 1d), with a particularly pronounced onset to the variability, south of the Davie Ridge at 17°S. Moorings at this location have revealed anticyclonic eddies moving through at a rate of about 4-5 per year (Ridderinkhof and de Ruijter, 2003). A hydrographic cruise at the time of the deployment revealed the existence of strong anticyclonic features on the western edge of the channel (Schouten et al., 2003); that survey did not cover the eastern side of the channel, where the variability is much weaker. Ocean colour data also confirm this southward train of anticyclonic eddies (Quartly and Srokosz, 2004). There is also a band of variability marking the EMC between 21° and 25°S, and heightened variability along 24°-26°S extending out to at least 75°E. These two bands, which are highlighted on Figs. 1c,d, are discussed in greater detail in section 3.2.

The region to the south and southwest of Madagascar is also marked by significant variability. This area of enhanced variability appears more constrained in the model output than in the altimetry, but variability maps for individual years (not shown) reveal changes in the patterns of eddy activity. To the southwest of Madagascar, the patch of high variability in the altimetry lies closer to the coast than that within OCCAM output. Ocean colour and infra-red imagery reveal large cyclonic eddies in this region (Quartly and Srokosz, 2004), which move west- or westsouthwestward; such features are only weakly present in OCCAM. AGAPE, a numerical model of the Indian Ocean also shows weak cyclonic activity here (Hermes et al., 2005).

3.2 Hovmöller diagrams of SSH

For the region east of Madagascar, the main axes of variability are along the EMC from 21°-25°S and along a band centred near 25°S (28°S in the model); these are highlighted in Figs. 1c,d. Hovmöller diagrams were constructed along these transects, sections of which are shown in Figs. 2 and 3. Both datasets show features heading southward along the EMC and westward along the zonal band. No direct matchup of individual events should be expected as, although the model has high-frequency atmospheric forcing, it will not be able to replicate the timing without assimilation of oceanographic data. Rather, here we are concentrating on the statistics (frequency of events, typical amplitude, speeds and interannual variability) describing the two datasets.

For the altimetry data, there are clear westward propagating signals along 25°S (Fig. 2b); the speed of the feature highlighted is 5.6 km day⁻¹ (6.5 cm s⁻¹). A 2-D Fourier transform of these data has a peak corresponding to a wavelength of 600 km and a period of 100 days, which corresponds to propagation at 6 km day⁻¹. East of 55°E, most of the features have roughly the same speed; however, there are several occasions when a feature remains relatively stationary for 2-3 months. This occurs near 51°E, and is the cause of the local peak in SSH variability there (Fig. 1c).

There is less regularity in the short section along the axis of the EMC (Fig. 2a). Examination of a number of features shows propagation rates varying between 3.7 and 14.1 km day⁻¹. Chapman et al. (2003) report ALACE floats at ~900 m depth in the EMC averaging 9.8 km day⁻¹ (with a standard deviation of ~6 km day⁻¹); their value refers to the mean current at depth, rather than the propagation rate of features within the EMC.

Earlier runs of OCCAM had shown greater levels of variability within the EMC than along the latitudinal band. This latest run, with high-frequency wind and latent heat forcing, matches the altimeter data better, in that it shows the stronger variability along the latitudinal band, albeit that it is located somewhat further south. The Hovmöller diagrams (Fig. 3) show that there is significant interannual variation. Figure 3a shows a number of features propagating southward along the axis of the EMC; the most pronounced anomalies occur during the first half of each year, when they are spaced approximately 45 days apart. The propagating signals for the latitudinal section (Fig. 3b) are present throughout the year. Typical propagation rates are 4 to 5.5 km day⁻¹, with a few features around July 1997 being retarded upon reaching 51°E.

3.3 Eddies or Rossby waves?

There is some uncertainty in the physical interpretation of the westward-moving features in Hovmöller diagrams, specifically the question as to whether the observations are of Rossby waves or a series of eddies – given that Rossby waves and a train of eddies may move at similar speeds. One important distinction between these two interpretations of Hovmöller diagrams (such as Figures 2 and 3) is that eddies transport water within their cores, whereas a propagating Rossby wave involves no zonal transport of water.

Some previous studies have categorised westward-propagating SSH features in the southern Indian Ocean as 'Rossby waves', but have often filtered the data to consider only annual or interannual signals. For example, the analysis of Schouten et al. (2002b) along 27°S used temporal filtering of SSH to produce a 3-month signal that was interpreted to be Rossby waves. Polito and Liu (2003) decomposed Hovmöller diagrams into nine separate components, four of which were different frequencies of Rossby waves. However, the resolution of their dataset did not allow them to consider the 3-month component as far south as 25°S. Intriguingly, their filter for the 'mesoscale eddy field' shows a clear but weak band around 25°S all the way from Australia to Madagascar (their Fig. 7). Morrow et al. (2004) show that anticyclones generated in the Leeuwin Current off Australia tend to head west-northwestwards up to 25°S, before propagating zonally; this could be the source of eddies in this band.

It may be possible to distinguish between Rossby waves and eddies by using extra information, in addition to SSH. Thus Quartly et al. (2003) and Challenor et al. (2004) examined Hovmöller diagrams of SSH, SST and ocean colour at 34°S and 32°S respectively, noting that SST led SSH by $\pi/2$ as would be expected for Rossby waves advecting water across a zonal temperature gradient. Examination of maps of SSH show features in this region with a meridional extent 1.5 to 3 times the zonal width (see top row of Fig. 4), which may indicate a wavefront rather than an eddy. However, these features are coherent enough that eddy-tracking techniques can be applied. Buck (2004) used a variant of the method of Isern-Fontanet et al. (2003) to identify and track these features in the vicinity of Madagascar. Additionally, the associated thermal anomalies (bottom row of Fig. 4) are not leading (i.e. directly to the west of) the height signatures as would be expected for Rossby waves. These results taken together suggest that the features are more likely to be eddies than Rossby waves.

Further insight may be gained by considering the secondary phytoplankton bloom, seen in ocean colour data, that occurs in late summer in some years to the east of Madagascar. Although advocating different mechanisms to explain the bloom, both Longhurst (2001) and Srokosz et al. (2004) note that an active eddy field is required to initiate and develop the bloom. Finally, we observe that in OCCAM (for which we have fields of true dynamic height as well as anomalies), the features along this band to the east of Madagascar appear to be primarily eddies. Therefore, we conclude that the observed features in the band around 25°S are probably eddies propagating

westwards, but acknowledge that more complex explanations may be possible – such as the instability of Rossby waves leading to their disintegration into eddies (LaCasce & Pedlosky, 2004). In this context, we note the recent results of Chelton et al. (2006) who use the method of Isern-Fontanet et al. (2003) to track eddies on a global scale in altimeter sea surface height data and distinguish these from Rossby waves. They conclude that at latitudes equatorward of 25° the westward propagation observed is due primarily to Rossby waves, while poleward of 25° it is due primarily to eddies. As our band of interest here centres on 25°S it is perhaps unsurprising that it has proved difficult to distinguish between Rossby waves and eddies as this is the transition zone between eddy and Rossby wave dominated regions.

3.4 Merging of eddies

The interaction of features propagating along the two highlighted lines is complicated. Figure 5 shows a series of altimeter composites for three separate occasions. We can see that even those features moving south in the EMC had originated from further east, with their westward movement and joining of the EMC mainly occurring at latitudes between 22° and 24°S. It is possible that these eddies have been formed by the diversion of some of the SEC around Réunion at the southern end of the Mascarene Ridge (Fig. 1a). However, those eddies are hard to follow along the Madagascan coast, as the anomalies appear to extend and contract along the direction of the strong current.

The westward-propagating eddies make regular progress along 25°S until they reach 51°E. This location, marked by locally increased variability (see Fig. 1c), acts as a 'parking place' where the eddies linger if progress is blocked by a feature to the west. Often a smaller feature from within the EMC will merge with the eddy (e.g. E with F and I with J in Fig. 5), and provide the necessary impetus to help the larger feature recommence its westward progress. At other times, the 'push' seems to come from other eddies queuing along the line to the east. A similar analysis of OCCAM output (not shown) also reveals eddies travelling along both axes and sometimes merging to the southeast of Madagascar.

4. Eddies and/or retroflection to the south of Madagascar

We now examine the mechanisms by which eddies can generate strong contrasts in ocean colour and infra-red satellite images, before moving on to re-consider the concept of an East Madagascar Retroflection.

4.1 Source of ocean colour and SST contrast

There is year-round coastal upwelling along the southern stretch of the EMC and in the shallower region just to the south of Madagascar. The upwelled waters are colder and richer in nutrients than the neighbouring surface waters. This latter factor leads to enhanced phytoplankton growth, with the result that recently upwelled waters can be detected using both their surface temperature and their colour.

The winds in the area are predominantly from the east, varying between northeast and southeast (Lutjeharms et al., 2000) and thus able to generate large variations in the degree of upwelling to the south of the island. The pattern at the southern end of the east coast has much less variation as it is principally caused by the shallowing bathymetry underlying the along-shore current (Lutjeharms and Machu, 2000). Cyclonic eddies occurring at the southwestern corner of Madagascar are made visible by the strands of high productivity waters that get wrapped around them, enabling them to be tracked as they move west or west-southwestwards towards the African mainland (Quartly and Srokosz, 2004). Here we concentrate on events to the south of the island, caused by eddies approaching along the routes discussed in sections 3.2.

Buck (2004) adopted the vorticity characterization of Isern-Fontanet et al. (2003) to define eddies within a region of possible current shear, and tracked such features (both cyclones and anticyclones) in the southwest Indian Ocean. Although there was much interannual variation, Buck

(2004) noted almost all features headed roughly westwards, although interaction with topography could lead to preferred directions ranging from northwesterly to southwesterly. In particular, he found that most eddies that had originated near the 25°S section subsequently crossed the Madagascar Ridge a few hundred kilometres south of Madagascar. Cyclonic and anticyclonic eddies in the EMC were harder to track automatically, but study of animations and sequences of images confirmed that such features do also pass to the south of Madagascar. The geostrophic flow field associated with eddies is such that the strongest offshore (southward) velocities will occur between a pair of eddies with the western one being a low (cyclone) and the eastern one a high (anticyclone). In many cases this strand of highly visible coastally-upwelled water is caught by the circulation of the anticyclonic eddy to the east, causing a temporary stream of high chlorophyll content waters towards the east.

Observations of a 'retroflexion' to the south of Madagascar are common, usually in single infra-red or ocean colour satellite images. The relatively warm waters of the EMC can be followed in sharply-defined arcs that resemble the behaviour of the Agulhas Retroflexion. Ocean colour data have provided many images of clearly delineated curves of high chlorophyll content waters. However, intriguingly, the EMC is itself low in nutrients and thus contains relatively few phytoplankton; the high productivity waters being imaged are those upwelled along the eastern and southern edges of Madagascar, which have subsequently been entrained along the edge of the EMC. As these represent deeper colder waters, they do not coincide with the warm arc of EMC waters seen in infra-red images.

In fact, features in this region often lose their thermal signatures quickly, whereas the ocean colour data continue to show a demarcation between water masses. We produced 10-day chlorophyll composites spanning September 1997 to May 2003. Sometimes there was considerable cloud cover or high levels of small scale variability so that no clear patterns of flow could be discerned. We then examined each of the clear composites to see whether there was an arc of high chlorophyll values that viewed in isolation gave the semblance of a retroflexion. This somewhat subjective assessment was made for each 10-day period, and a record kept of whether any composite in each individual month showed patterns indicative of an apparent retroflexion (Fig. 6). Approximately half the months contained such imagery, with the appearance of a retroflexion occurring for nearly every February. This does not imply that the feature is more common than in other months, but that the biological conditions are such as to optimise its detection via ocean colour sensors.

4.2 The retroflexion reconsidered

However, study of sequences of images suggests behaviour other than retroflexion. Quartly and Srokosz (2003b) show a series of SeaWiFS composites that are more consistent with the idea of an anticyclonic eddy propagating southwards through the region. Lutjeharms and van Ballegooyen (1988) show a schematic for the westward progradation of the Agulhas Retroflexion, with interaction between the neighbouring opposing flows of the Agulhas Current and Agulhas Return Current leading to an eastward retraction of the retroflexion and the pinching off of an Agulhas ring. No such behaviour is observed for the EMC, with the anticyclonic feature moving westward without the reformation of a loop to its east.

We consider three specific case studies showing an apparent retroflexion in the SeaWiFS imagery (Fig. 7), and examine the contemporaneous altimeter data to provide insight concerning the changing currents. (Recall that SSH anomaly fields cannot reveal a mean flow.) Rather than selecting examples that best match our hypothesis of propagating eddies to the southwest of Madagascar, the examples chosen coincide with ocean colour or infra-red SST imagery already published in support of the concept of an East Madagascar Retroflexion. The 10-day composite in Fig. 7c covers the event depicted in Fig. 1b of Lutjeharms and Machu (2000); Fig. 7f spans Figs. 2e-f of di Marco et al. (2000); and Figs 7i,j,k replicate the series shown in Figs. 2g-i of Quartly and Srokosz (2003a). All three of these papers (including our earlier paper) accepted the prevailing idea of the existence of an East Madagascar Retroflexion.

The altimetry data are challenging to understand, because they only provide height (and thus currents) relative to some unknown mean which may be expected to have sharp gradients in this region, and also the applied interpolation may not give a clear representation of features moving across tracks within the period of compilation. The first series (Fig. 7a-d) shows a region of high SSH (A) elongated along the southeast coast of Madagascar. As this heads southwestward through the region south of Madagascar, it wraps a clearly-defined strip of highly productive waters anticyclonically around it, the sharpness of the feature being enhanced by the cyclone (B) at 47°E, 28°S (Fig. 7c).

Similarly in Fig. 7f, the development of a southward shaft of low productivity waters coincides with a slight SSH high (C) at 46°E, 27°S indicating anticyclonic circulation. The SSH feature then heads southwestward, accompanied by a patch of low chlorophyll concentration waters, with another feature developing at 48°E, 26°S (Fig. 7h). The third case shows a large anticyclone at 50°E, 27°S splitting, with the western portion merging with a smaller feature within the EMC to create a local SSH high at 46°E, 26°S (X in Fig. 7k) that produces some eastward flow at its southern limit. This feature then moves southwestward from the region, although the coverage by SeaWiFS is poor for the ensuing 10-day period (Fig. 7l). Gründlingh (1995) had earlier noted eddies heading westward over the Madagascar Ridge, and de Ruijter et al. (2004) commented upon the intermittent existence of eddy pairs there, with the anticyclonic component usually heading west or southwestward.

Could this scenario (anticyclonic eddies propagating to the south of Madagascar) offer an alternative explanation to the 'East Madagascar Retroflexion' for explaining the observed behaviour of currents in this region? Certainly, problems exist with the hypothesis that the East Madagascar Current retroflects. The retroflexions of the Agulhas and North Brazil Currents feed well-documented persistent eastward currents; there does not appear to be such a current at 25°S-28°S in the Indian Ocean (see, for example, Stramma and Lutjeharms, 1997), although de Ruijter et al. (2004) argue that a localized retroflexion could exist spawning eddies. The compilation of ship drift data by Lutjeharms et al. (2000) show no consistent eastward flow; and the average wind field in the region is to the west, with the zero in the wind stress curl lying much further to the south.

This area has been only rarely sampled by ships or drifting buoys. Lutjeharms et al. (1981) show the tracks of some surface drifters that passed through that region in the 1970s. The extensive catalogue of data gathered together by the WOCE project only includes 15 such buoys during 1995-2000 passing through the area just to the southeast of Madagascar, and more than half of those were within a 6-month period in 2000. Their trajectories (Fig. 8a) weave a complex web, but some patterns can be discerned. All tracks are plotted from the moment when a drifter heads south of 25°S along the EMC. Two drifters do loop back to locations further northeast. However, the majority of the remaining tracks pass close to the south of the island, with two of them looping anticyclonically around point A (a seamount at the end of a southeastward jutting spur, see Fig. 1a), then heading northwards for a while along 48°E (the eastern flank of the Madagascar Ridge), before reversing and heading south again at that longitude. Another buoy loops once around A cyclonically. Of the 15 detected within the main EMC, three exit the region towards the east at 25°S, three leave the region plotted at the southeast corner, and the remaining nine cross the ridge, although not all subsequently join the Agulhas Current. Two buoys initially head northwards up the eastern side of the Mozambique Channel, before returning on the western side. It is likely that these were caught by strong cyclonic flow to the southwest of Madagascar (see Quartly and Srokosz, 2004). These two buoys were in May 1996 and May 2000, but the number of events is insufficient for determining clear seasonal differences. The general pattern of ALACE float trajectories at 900 m depth shows a westward progression (Chapman et al., 2003), although the authors thought that one of the floats underwent a retroflexion.

Virtual drifters released in OCCAM have a somewhat simpler envelope of trajectories (Fig. 8b). A few diverge strongly from the westward path, including some heading northeastwards out

of the EMC; however, the majority of the drifters execute one or more anticyclonic loops to the south of Madagascar, and then continue on towards the Agulhas Current.

Altimetry provides a measure of the temporal changes in the flow, but cannot presently give the mean transport. To put these anomalies in context, we look at absolute transports within OCCAM. We have analysed the full 18 years of the latest OCCAM run, calculating transport across six sections radiating eastward to southward from Madagascar (Fig. 9). The calculations confirm a poleward-flowing EMC, increasing in transport from 5.1 Sv at 20°S to 14.8 Sv at 24°S, with 29.1 Sv in total flowing around the south of the island. Other numerical models have given similar results — POCM having 30 Sv flowing south of the island (Matano et al., 2002), and transport in AGAPE increasing from 7 Sv at 20°S to 16 Sv at 25°S, with 35 Sv rounding the island (Hermes et al., 2005). There have been few hydrographic sections in this region. Swallow et al. (1988) determined a flow of 22.5 Sv at 23°S in April 1985, but noted that up to 7 Sv of that could be due to an offshore eddy. They also quoted previous transport estimates for that latitude ranging from 16.6 to 23.7 Sv. Donohue and Toole (2003) determined a transport of 19.3 Sv at 25°S for the WOCE I4E section taken in June 1995, and a surprisingly higher transport of 21.6 Sv further north at 20°S

Time series of OCCAM transport for each of the sections show much variability, especially over short time scales. We determined the standard deviation of the transports (given in parentheses in Fig. 9); these give an indication of the importance of mesoscale processes to the flow, and suggest the likely uncertainty in transport from one-time hydrographic surveys. We particularly note that OCCAM shows 5.1 Sv entering from the east between 24°S and 29.25°S, with eddy variability causing a standard deviation significantly greater than the mean.

While the transport in OCCAM is clearly westward, both to the east and south of Madagascar (Fig. 9) consistent with observations, the near-surface current field does not show such a simple structure. The model results (not shown) suggest that there may be some flow to the east at ~25-28°S, but this is confounded with the intermittent eastward flows generated by rotating eddies. A more detailed investigation of the OCCAM model results is being undertaken and will be reported elsewhere.

5. Summary

This paper has looked at the variability in sea surface height in the southwest Indian Ocean, its representation in a high-resolution numerical model, and at what information both satellite and model can give us on the currents to the south of Madagascar. Many analyses of mesoscale variability from altimetry have shown the patch of high variability to the southwest of Madagascar, associated with the movement of eddies in that region. We also find bands of relatively high variability along 25°S and along the East Madagascar Current. These features were present in the original data (Fig. 1b), but the clarity of the 'eddy corridor' at 25°S was improved by our spatiotemporal filtering (Fig. 1c) which removes large-scale coherent variations from the SSH fields. Our work complements that of Schouten et al. (2002a), who also find a meridional band, by using a restrictive band-pass filter based on a frequency of 4 cycles per year. They refer to their signals as being manifestations of Rossby waves, but it is possible that the propagating features that we note in Fig. 2b are a mixture of eddies and Rossby waves. We draw particular attention to the variability peak at 51°E, 25°S, which acts as a 'parking place' for eddies along their westward journey. It is possible that many of the eddies may have originated in the Leeuwin Current off the west coast of Australia, and then headed slightly equatorward (Morrow et al., 2004), although it is not clear why they should then congregate at 25°S. Altimetric features within the EMC are harder to resolve, and a Hovmöller diagram (Fig. 2a) shows features travelling at a range of speeds and durations. Examination of series of plots of SSH anomaly do show eddies moving west to join the EMC at latitudes between 22° and 24°S.

Many of the general observations from altimetry are echoed in the analysis of output from OCCAM, which shows that the model is getting the pattern of short-term variability correct.

However, the amplitude of the SSH signals in OCCAM is still a little weaker than that shown in the altimetry, with the zonal band of SSH variability being located somewhat further south. The model shows a clear train of anticyclonic eddies heading southward from 21°S, which appear to be generated by flow past Réunion and Mauritius. Biastoch and Krauss (1999) noted that their eddy-permitting regional model had large variability within the EMC (due to a series of southward bound anticyclonic eddies), but minimal indication of features heading westward across the Indian Ocean at 25°S. An earlier run of OCCAM, with different vertical resolution and forcing terms also showed greater variability within the EMC than along the zonal band. Biastoch and Krauss (1999) refer to the need for realistic yet smoothed topography, but note that passages need to be at least two grid cells wide to allow inter-basin flow. The bathymetry along the Madagascar Ridge is quite shallow, with various seamounts rising to within 1000m of the surface. This may explain why the initial swarm of trajectories followed by WOCE drifters around the southeast corner of Madagascar and then confined between point A and the shelf of the island (Fig. 8a) appears more channelled than in the model. (Fig. 8b) The train of anticyclonic eddies in OCCAM transport nearly all the virtual drifters across to the Agulhas Current, whereas a greater variety of paths are followed by the WOCE drifters, including two heading north on the eastern side of the Mozambique Channel.

The fate of the waters of the East Madagascar Current has long been a subject of interest, with three alternatives having been suggested previously: northbound up the west coast of Madagascar, directly westward to the Agulhas Current, or eastward following the retroflexion model of the Agulhas Current. Clearly drifters, one-time hydrographic surveys and single satellite images may show momentary realizations of all of these, but does any consistent pattern of flow exist? Consider the first alternative, that of the current turning northward and hugging the coast of Madagascar before crossing the Mozambique Channel further up. Two of the drifters (see Fig. 8a) do head north in the Mozambique Channel, but do not stay close to the coast. Their paths are more consistent with them being caught temporarily by the cyclonic eddies found to the southwest of Madagascar (Quartly and Srokosz, 2004). In addition, di Marco et al. (2000) show evidence of southbound jets of warm water along this part of the coast. Thus the view that the East Madagascar Current turns persistently northward along the coast does not seem tenable.

The second alternative, that of the East Madagascar Current simply heading due west to the Agulhas Current seems ruled out by both the results of de Ruijter et al. (2004) and our results here. These show the abundance of eddy features in this area and the apparent lack of a steady current to the west. Models (e.g. Biastoch and Krauss, 1999) and ship drift data (Lutjeharms et al., 2000) show the mean surface flow to be to the west. Occasional images from SeaWiFS show a tendril of chlorophyll stretched almost due west, but it is more common for drifters to follow a circuitous route across the Mozambique Basin, as caught in eddies showing both cyclonic and anticyclonic flow. Some of these eddies reach the Agulhas Current and are absorbed into it.

The third alternative, that of a persistent retroflexion, like that of the Agulhas, is also ruled out by both the results of de Ruijter et al. (2004) and our results here. There is no obvious wind field nor buoyancy forcing to engender long-term eastward flow at 25°-30°S (as noted by de Ruijter et al., 2004; who concentrated on the intermittently occurring pairs of cyclonic and anticyclonic eddies – dipoles – whereas we have been considering the more general behaviour of eddies in this region). Thus we conclude that no persistent retroflexion exists in the region. The transitory small-scale recirculation toward the east, seen in satellite SST and ocean colour images, is explained by an anticyclone moving through the region, wrapping both the warm East Madagascar Current waters and the nutrient-rich upwelled waters into the well-defined arcs. Occasionally strands of chlorophyll-rich water can stretch 500 km or more eastward but such apparent meanderings of an eastward current are readily explained by the extrusion and contortion of a chlorophyll strand by a combination of the effects of both cyclonic and anticyclonic eddies.

In summary, several high-resolution numerical models agree that there is a net transport of order 30 Sv around the south of Madagascar. Some of this flow regime involves large anticyclonic eddies, with temporary recirculation towards the east, but with no persistent retroflexion or

eastward-flowing return current – unlike the Agulhas. The time series for the southern section in OCCAM (not shown) indicates that the transport varies between 20 and 40 Sv, consistent with a persistent westward flow plus eddies. Indeed, a small proportion of the drifters pass through the region without getting caught in eddies. During a recent research cruise (February 2005) we have deployed moorings south of Madagascar, which will help us to determine the actual mean flow in this region.

Acknowledgements

The altimetry data used were the Mean Sea Level Anomaly product produced by CLS as part of the EU projects AGORA and DUACS, and the ocean colour data were based on SeaWiFS data distributed by NASA/GSFC. The TMI data are processed and provided by Remote Sensing Systems, sponsored by NASA's Earth Science Information Partnerships (ESIP). Drifter data were obtained from a compilation on the DVD *WOCE Global Data v3.0*. We are grateful to Paolo Cipollini for discussions on Rossby waves, and to the OCCAM team for access to the model output; details of the model and animation for the Agulhas region may be found at <http://www.noc.soton.ac.uk/JRD/OCCAM>.

References

- Beal, L. M., Bryden, H. L., 1999. The velocity and vorticity structure of the Agulhas Current at 32°S. *J. Geophys. Res.*, 104, C3, 5151-5176.
- Biastoch, A., Krauss, W., 1999. The role of mesoscale eddies in the source regions of the Agulhas Current. *J. Phys. Oceanogr.*, 29, 2303-2317.
- Buck, J. J. H., 2004. Eddies in the East Madagascar Current. [MSc dissertation, available from National Oceanography Centre, Southampton, UK].
- Campbell, J. W., 1995. The lognormal distribution as a model for bio-optical variability in the sea. *J. Geophys. Res.*, 100, 13237-13254.
- Challenor, P. G., Cipollini, P., Cromwell, D., Hill, K. L., Quartly, G. D., Robinson, I. S., 2004. Global characteristics of Rossby wave propagation from multiple satellite datasets. *Int. J. Rem. Sens.*, 25 (7-8), 1297-1302.
- Chapman, P., di Marco, S. F., Davis, R. E., Coward, A. C., 2003. Flow at intermediate depths around Madagascar based on ALACE float trajectories. *Deep-Sea Res. II*, 50, 1957-1986.
- Chelton, D. B., Schlax M. G., Samelson R. M., de Szoeke R. A., 2006. Global observations of westward energy propagation in the ocean: Rossby waves or eddies? submitted to *Science*. (available from ftp://numbat.coas.oregonstate.edu/pub/chelton/eddies/chelton_etal_2006_science_submitted.pdf)
- Coward, A. C., de Cuevas, B. A., 2005. The OCCAM 66 level model: Model description, physics, initial conditions and external forcing. SOC Internal Report no. 99. [available from National Oceanography Centre, Southampton, UK]
- de Cuevas, B. A., Webb, D. J., Coward, A. C., Richmond, C. S., Rourke, E., 1999. The UK Ocean Circulation and Advanced Modelling Project (OCCAM). pp 325-335 in *High Performance Computing, Proceedings of HPCI Conference 1998, Manchester, 12-14 January 1998*, R.J. Allan, M.F. Guest, A.D. Simpson, D.S. Henty, D.A. Nicole (Eds) Plenum Press.
- de Ruijter, W. P. M., Boudra, D. B., 1985. The wind-driven circulation in the South Atlantic-Indian Ocean - I. Numerical experiments with a one-layer model. *Deep-Sea Res.*, 32, 557-574.
- de Ruijter, W.P.M., Biastoch, A., Drijfhout, S.S., Lutjeharms, J.R.E., Matano, R.P., Pichevin, T., van Leeuwen, P.J., Weijer, W., 1999. Indian-Atlantic interocean exchange: Dynamics, estimation and impact. *J. Geophys. Res.*, 104 (C9), 20885-20910.
- de Ruijter, W. P. M., van Aken, H. M., Beier, E. J., Lutjeharms, J. R. E., Matano, R. P., Schouten, M. W., 2004. Eddies and dipoles around South Madagascar: formation, pathways and large-scale impact. *Deep-Sea Res. I*, 53 (3), 383-400.

- di Marco, S. F., Chapman, P., Nowlin, W. D., 2000. Satellite observations of upwelling on the continental shelf south of Madagascar. *Geophys. Res. Lett.*, 27, 3965-3968.
- Donohue, K. A., Toole, J. M., 2003, A near-synoptic survey of the Southwest Indian Ocean. *Deep-Sea Res. II*, 50, 1893-1931.
- Gründlingh, M. L., 1993. On the winter flow in the southern Mozambique Channel. *Deep-Sea Res.*, 40 (2), 409-418.
- Gründlingh, M. L., 1995. Tracking eddies in the southeast Atlantic and southwest Indian oceans with TOPEX/POSEIDON. *J. Geophys. Res.*, 100, 24977-24986.
- Hermes, J. C., Reason, C. J. C., Lutjeharms, J. R. E., 2005. Modelling the variability of the source regions of the Agulhas Current. submitted to *J. Climate*.
- Isern-Fontanet, J., Garcia-Ladona, E., Font, J., 2003. Identification of marine eddies from altimetric maps. *J. Atmos Oceanic Tech.*, 20 (5), 772-778.
- LaCasce, J. H., Pedlosky, J., 2004. The instability of Rossby basin modes and the oceanic eddy field. *J. Phys. Oceanogr.*, 34, 2027-2041.
- Le Traon, P.-Y., Ogor, F., 1998. ERS-1/2 orbit improvement using TOPEX/POSEIDON: The 2cm challenge. *J. Geophys. Res.*, 103 (C4), 8045-8057.
- Le Traon, P.-Y., Nadal, F., Ducet, N., 1998. An improved mapping method of multisatellite altimeter data. *J. Atmos Oceanic Tech.*, 15 (2), 522-534.
- Longhurst, A., 2001. A major seasonal phytoplankton bloom in the Madagascar Basin. *Deep-Sea Res. I*, 48, 2413-2422.
- Lutjeharms, J. R. E., 1976. The Agulhas Current system during the northeast monsoon. *J. Phys. Oceanogr.*, 6, 665-670.
- Lutjeharms, J. R. E., 1988. Remote sensing corroboration of retroflexion of the East Madagascar Current. *Deep-Sea Res.*, 35, 2045-2050.
- Lutjeharms, J. R. E., Machu, E., 2000. An upwelling cell inshore of the East Madagascar Current. *Deep-Sea Res.*, 47, 2405-2411.
- Lutjeharms, J. R. E., van Ballegooyen, R. C., 1988. The retroflexion of the Agulhas Current. *J. Phys. Oceanogr.*, 18, 1570-1583.
- Lutjeharms, J. R. E., Bang, N. D., Duncan, C. P., 1981. Characteristics of the currents east and south of Madagascar. *Deep-Sea Res.*, 28A, 879-899.
- Lutjeharms, J. R. E., Wedepohl, P. M., Meeuwis, J. M., 2000. On the surface drift of the East Madagascar and Mozambique Currents. *S. African J. Sci.*, 96, 141-147.
- Matano, R. P., Beier, E. J., Strub, P. T., Tokmakian, R., 2002. Large-scale forcing of the Agulhas variability: The seasonal cycle. *J. Phys. Oceanogr.*, 32, 1228-1241.
- Morrow, R., Birol, F., Griffin, D., Sudre, J., 2004. Divergent pathways of cyclonic and anti-cyclonic ocean eddies. *Geophys. Res. Lett.*, 31, L24311, doi:10.1029/2004GL020974.
- Polito, P.S., Liu, W.T. 2003. Global characterization of Rossby waves at several spectral bands. *J. Geophys. Res.*, 108, 3018, doi: 10.1029/2000JC000607.
- Quartly, G. D., Srokosz, M. A., 1993. Seasonal variations in the region of the Agulhas Retroflexion: Studies with Geosat and FRAM. *J. Phys. Oceanogr.*, 23, 2108-2124.
- Quartly, G. D., Srokosz, M. A., 2002. SST observations of the Agulhas and East Madagascar Retroflexions by the TRMM Microwave Imager. *J. Phys. Oceanogr.*, 32, 1585-1592.
- Quartly, G. D., Srokosz, M. A., 2003a. Satellite observations of the Agulhas Current System. *Phil. Trans. Roy. Soc. Lond. A*, 361, 51-56.
- Quartly, G. D., Srokosz, M. A., 2003b. A Visible Record of Eddies in the Southern Mozambique Channel. *Proc. of IGARSS 2003 21st-25th July 2003, Toulouse, France* (3pp).
- Quartly, G. D., Srokosz, M. A., 2004. Eddies in the southern Mozambique Channel. *Deep-Sea Res. II*, 51 (1-3), 69-83.
- Quartly, G. D., Cipollini, P., Cromwell, D., Challenor, P. G., 2003. Rossby waves: Synergy in action. *Phil. Trans. Roy. Soc. Lond. A*, 361, 57-63.
- Ridderinkhof, H., de Ruijter, W. P. M., 2003. Moored current observations in the Mozambique Channel. *Deep-Sea Res. II*, 50 (12-13), 1933-1955.

- Schott, F., Fieux, M., Kindle, J., Swallow, J., Zantopp, R., 1988. Boundary currents east and north of Madagascar. 2. Direct measurements and model comparisons. *J. Geophys. Res.*, 93, 4963-4974.
- Schouten, M. W., de Ruijter, W. P. M., van Leeuwen, P. J., Dijkstra, H. A., 2002a. An oceanic teleconnection between the equatorial and southern Indian Ocean. *Geophys. Res. Lett.* 29 (16), art. no. 1812.
- Schouten, M. W., de Ruijter, W. P. M., van Leeuwen, P. J., 2002b. Upstream control of Agulhas Ring shedding. *J. Geophys. Res.* 107 (C8), art. no. 3109. doi: 10.1029/2001/JC000804.
- Schouten, M. W., de Ruijter, W. P. M., van Leeuwen, P. J., Ridderinkhof, H., 2003. Eddies and variability in the Mozambique Channel. *Deep-Sea Res. II*, 50 (12-13), 1987-2003.
- Srokosz, M. A., Quartly, G. D., Buck, J. J. H., 2004. A possible plankton wave in the Indian Ocean. *Geophys. Res. Lett.* 31, L13301. doi:10.1029/2004GL019738.
- Stramma L., Lutjeharms, J. R. E., 1997. The flow field of the subtropical gyre of the South Indian Ocean. *J. Geophys. Res.*, 102, 5513-5530.
- Swallow, J., Fieux, M., Schott, F., 1988. The boundary currents east and north of Madagascar 1. Geostrophic currents and transports. *J. Geophys. Res.*, 93, 4951-4962.
- Tomczak, M., Godfrey, J. S., 1994. *Regional oceanography: An introduction*. Pergamon, 422 pp.
- Webb D.J., de Cuevas, B. A., Coward, A. C., 1998. The first main run of the OCCAM Global Ocean Model. Southampton Oceanography Centre, Internal document no. 34. [available from National Oceanography Centre, Southampton, UK]

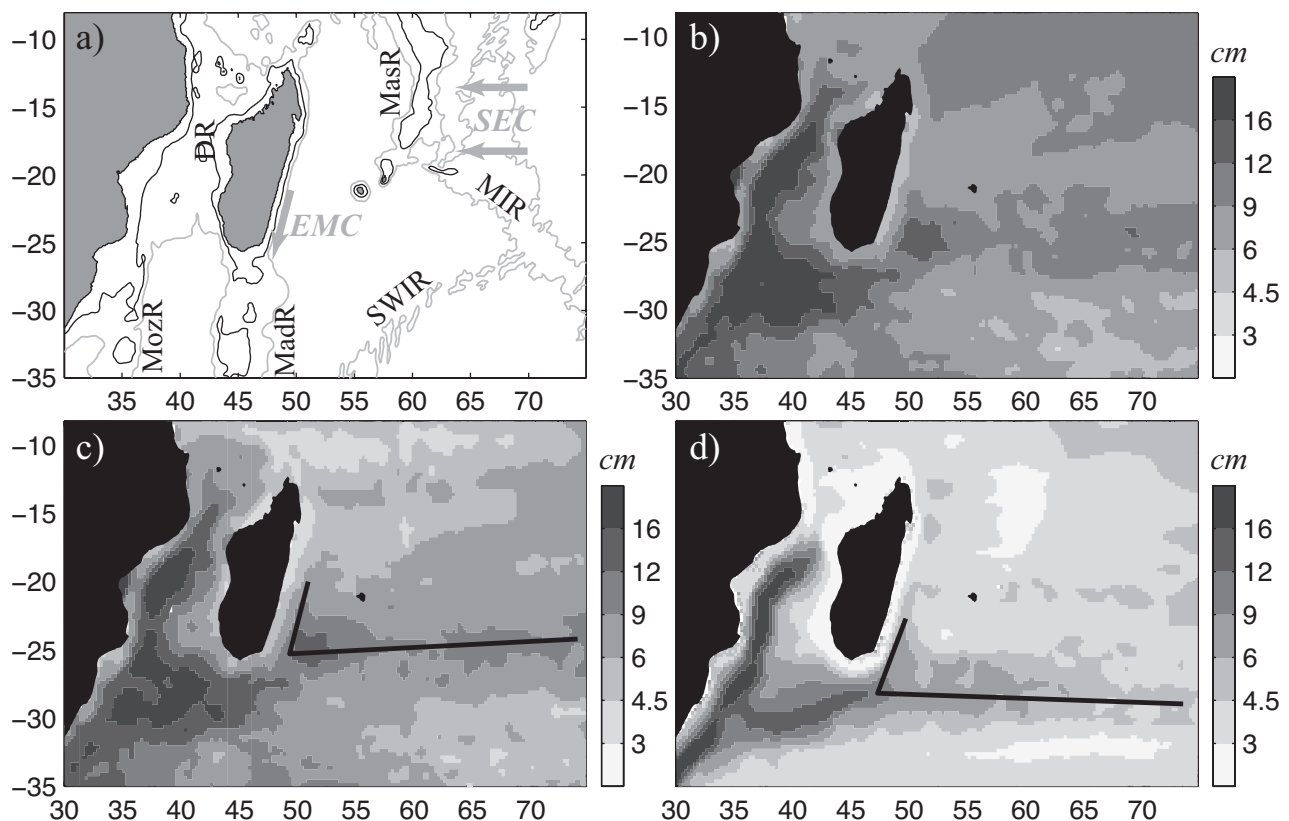


Figure 1 : a) Bathymetry of southwest Indian Ocean with main currents overlaid. (thick contour = 2500m, thin contour = 1000m, MozR - Mozambique Ridge, MadR - Madagascar Ridge, DR - Davie Ridge, MasR - Mascarene Ridge, MIR - Mid-Indian Ridge, SWIR - Southwest Indian Ridge, SEC - South Equatorial Current, EMC - East Madagascar Current) b) R.m.s. SSH variability from altimetry, c) R.m.s. SSH variability from altimetry after 4 most significant EOF modes removed. d) R.m.s. variability of OCCAM output after 4 most significant EOF modes removed. The straight lines marked on c, d are the sections used for Hovmöller analysis later in the paper.

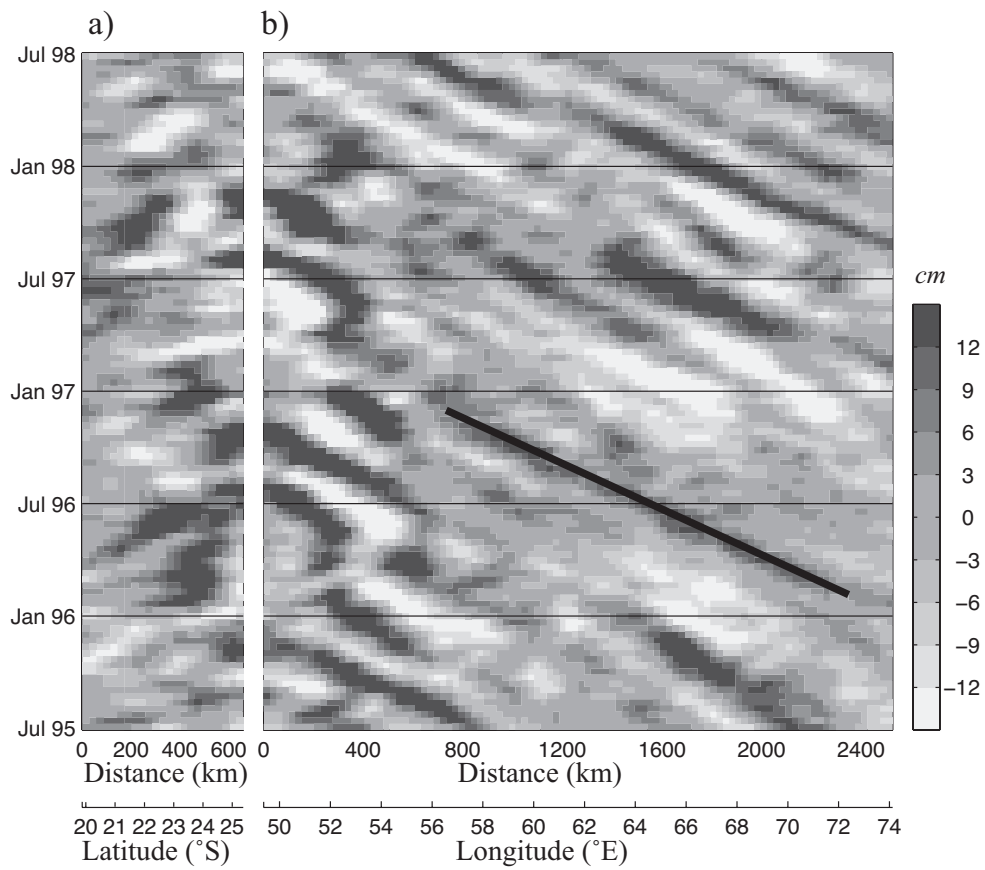


Figure 2 : Hovmöller diagrams of filtered altimetry along a) EMC axis, b) approximate 25°S line.

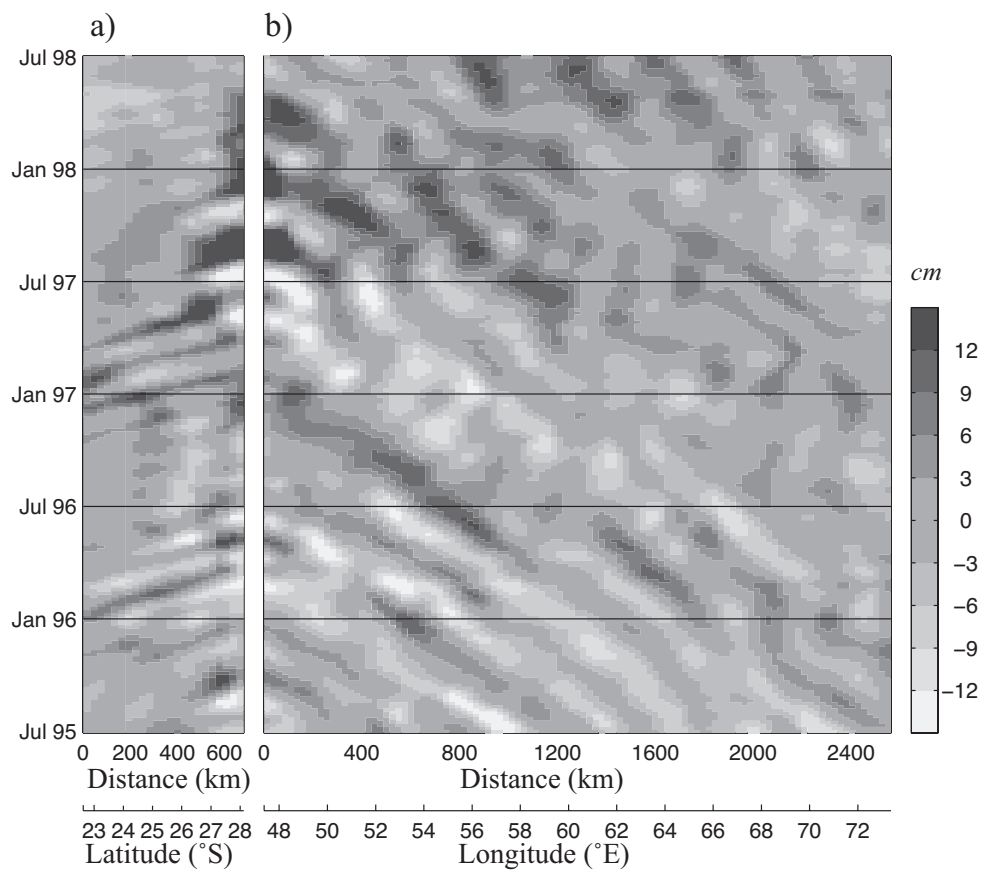


Figure 3 : Hovmöller diagrams of filtered OCCAM output along a) EMC axis, b) approximate 27°S line.

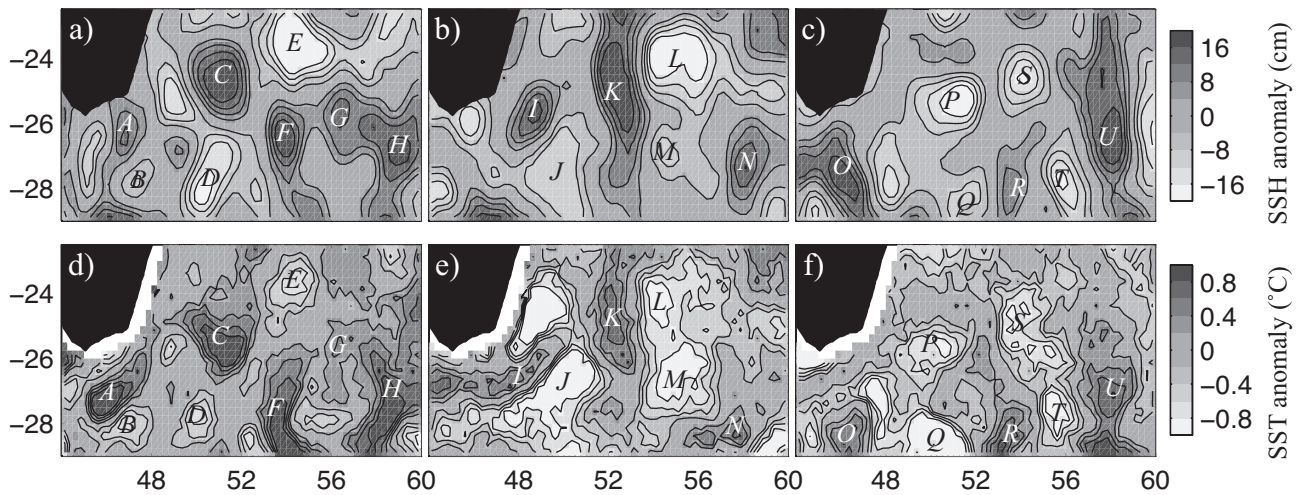


Figure 4 : Three separate time epochs showing similarity of signal between 10-day snapshots of SSH anomaly from altimetry (top row) and SST from TMI (bottom row). a,d) mid-August 1998, b,e) mid-May 1999, c,f) mid-October 2000. The capital letters identify features in common.

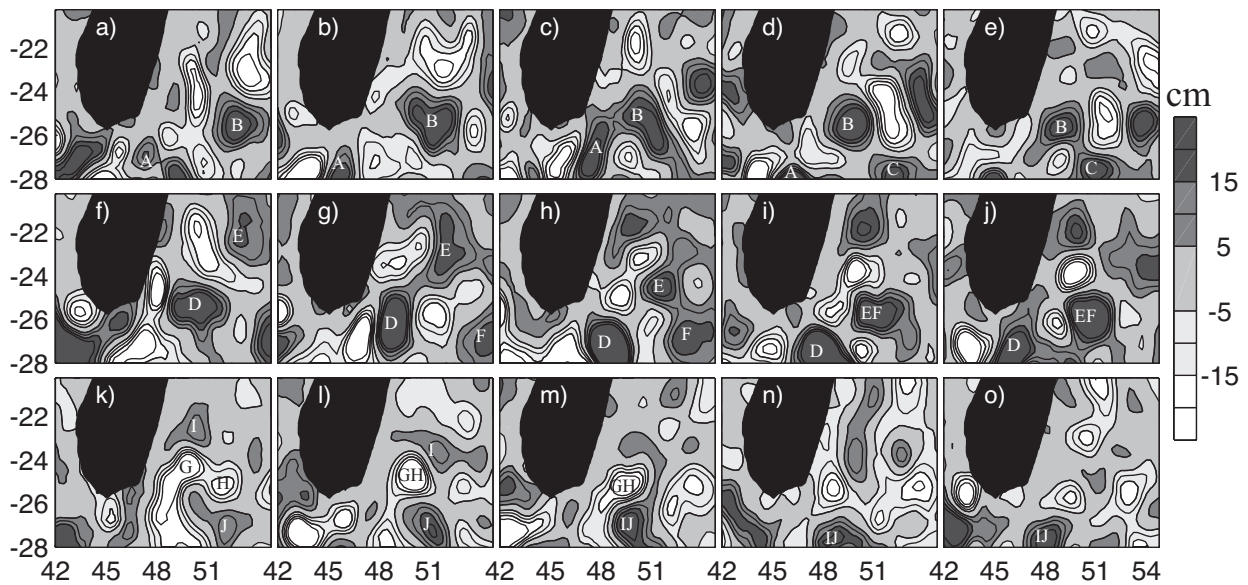


Figure 5 : Eddy propagation southeast of Madagascar as shown by altimetry. Three separate series, with 20-day intervals between successive images in each of a-e), f-j) and k-o). Some anomalies propagate westward around 22°S to join the EMC, but are then hard to follow as they move south. The capital letters identify individual features, showing their interaction, with some merging but others remaining separate.

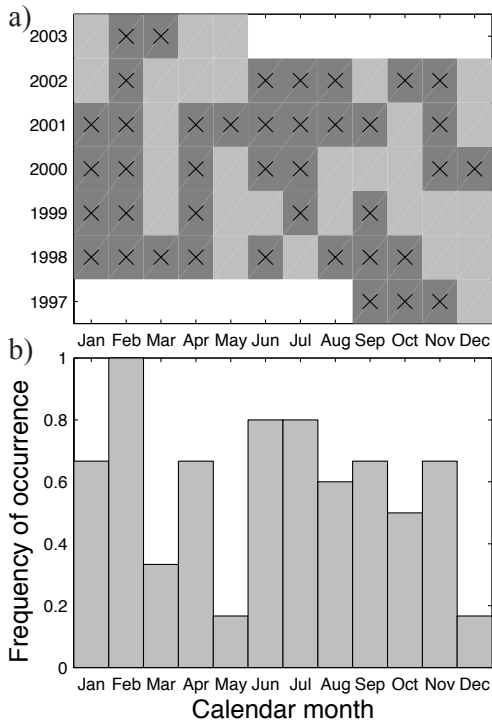


Figure 6 : a) Tally of months when a possible 'retroflexion' can be observed in SeaWiFS data. Shaded regions indicate months for which data were available; dark shading with 'X' superposed indicates retroflexion-like signal apparent. b) Likelihood associated with each calendar month. (Note lack of clear signal in ocean colour data does not necessarily mean that no circulation feature is present.)

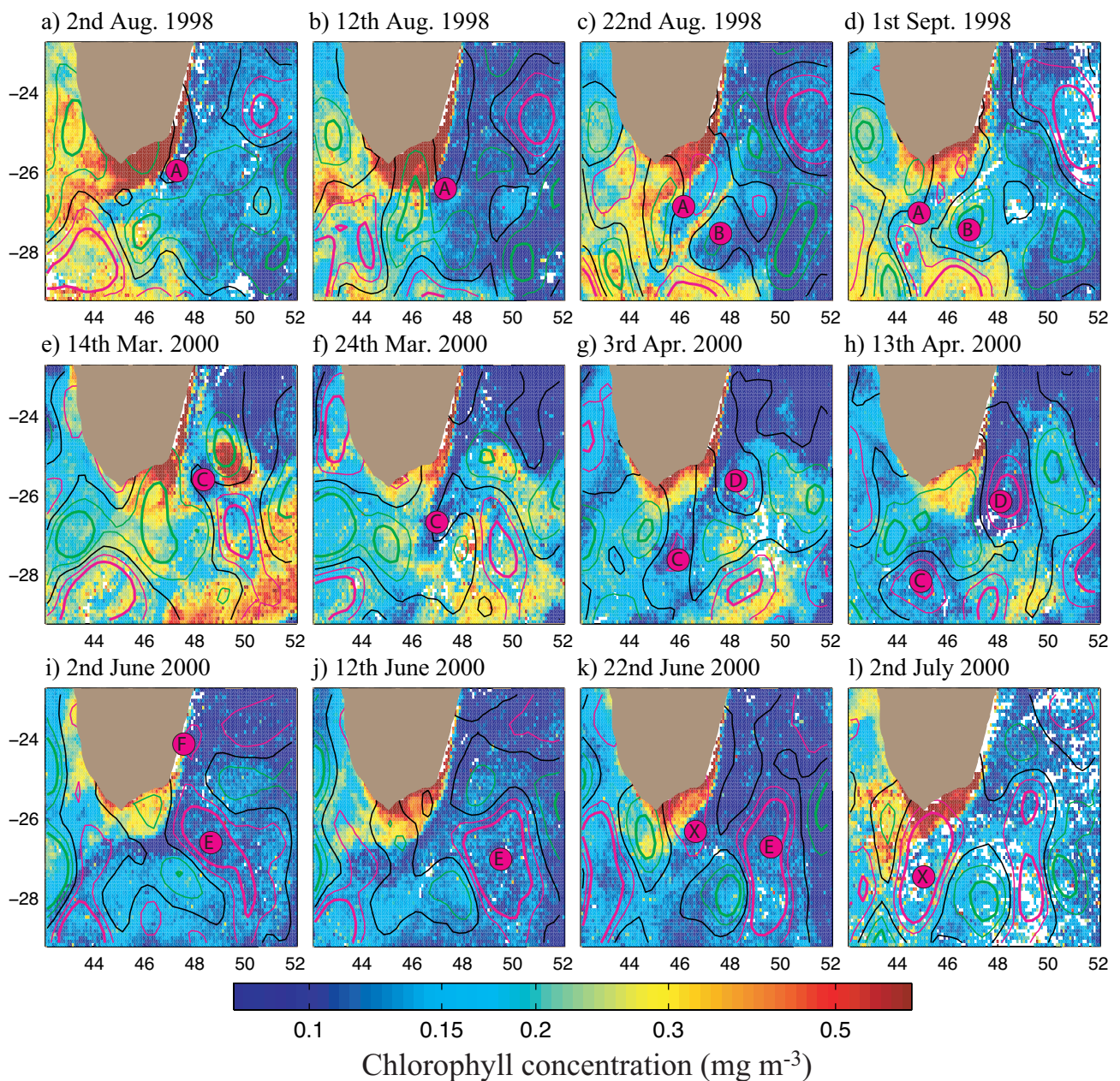


Figure 7 : Reappraisal of ocean colour imagery previously published as evidence of an East Madagascar Retroflection. Each row shows consecutive 10-day composites of chlorophyll values, with the contemporaneous filtered SSH superimposed (contours are at intervals of 7 cm, with the pink lines representing positive features and the green lines negative ones) a-d) August 1998, covering the event detailed in Lutjeharms and Machu (2000); e-h) March-April 2000 spanning the period illustrated by di Marco et al. (2000); i-l) June 2000, replicating the series shown by Quartly and Srokosz (2003a). The key SSH features are indicated by the symbols letters, with X representing the merger of F with part of E; the features are not always marked by a large absolute value, but are high relative to immediate region. The most productive waters are just south of Madagascar, fuelled by upwelled nutrient-rich water; all productivity further from the island are due to a combination of local upwelling caused by eddies and, more importantly, the advection of upwelled coastal waters around eddy features.

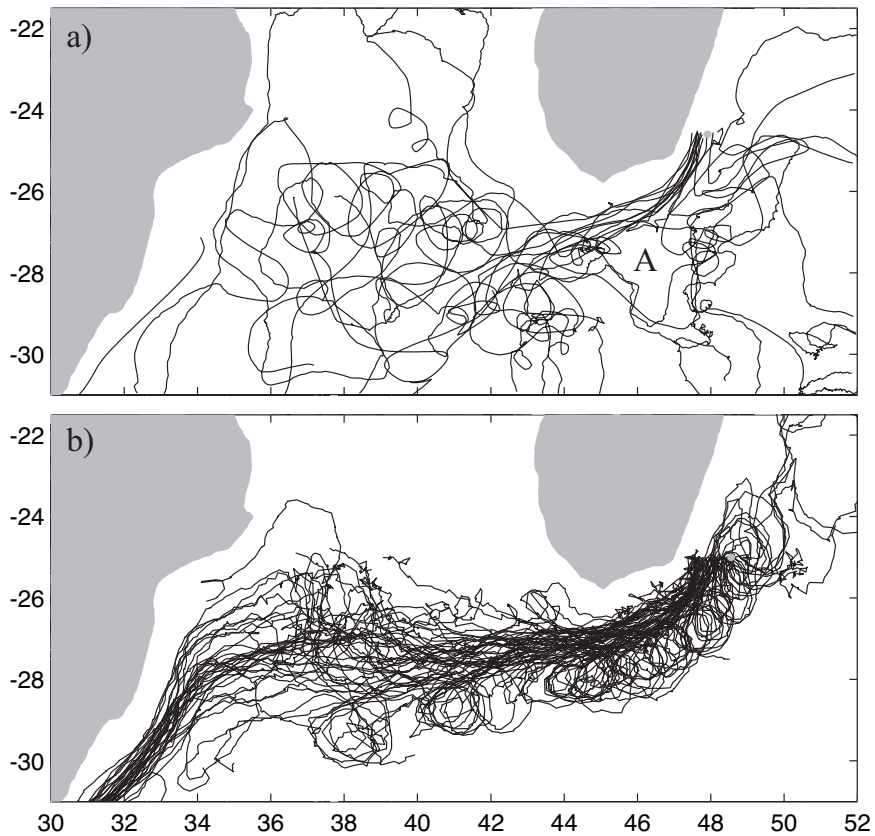


Figure 8 : Trajectories of drifters passing 25°S within the East Madagascar Current. a) Compilation of WOCE drifters from 1995-2000. Drifters plotted from when they pass 25°S within the EMC (start points marked by grey dots). For discussion of point A, see text. b) Virtual floats released in OCCAM. Compilation of various times of release and locations (marked by grey dots) across EMC at 25°S.

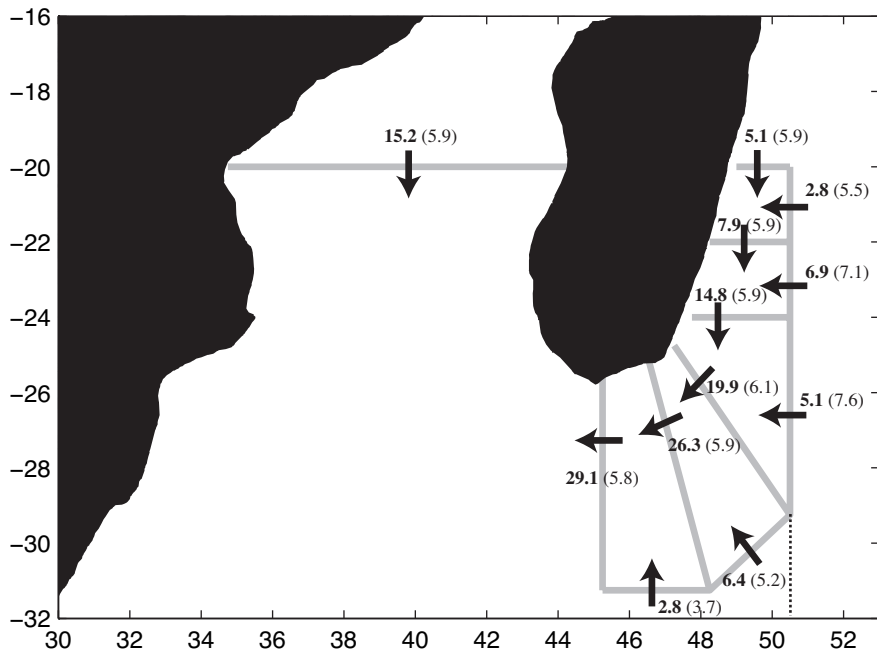


Figure 9 : Transports across various sections in the OCCAM run. The first figure gives the mean transport (in Sv) for the 18-year period, with the standard deviation in parentheses. Note, this is not an uncertainty in the mean, but a measure of the variability in the flow.